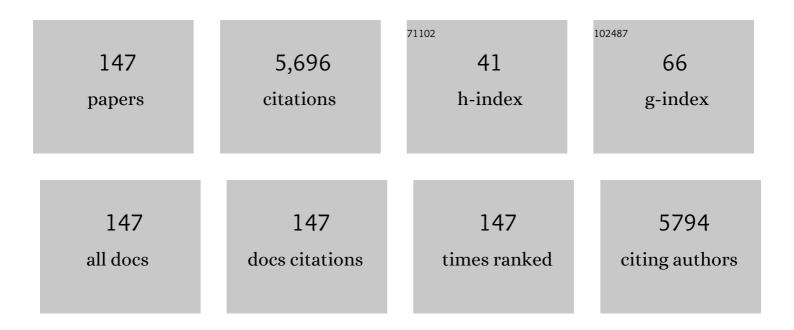
List of Publications by Year in descending order

Source: https://exaly.com/author-pdf/606206/publications.pdf Version: 2024-02-01



HAI-HONG WU

#	Article	IF	CITATIONS
1	Highly Site-Selective Direct C–H Bond Functionalization of Phenols with α-Aryl-α-diazoacetates and Diazooxindoles via Gold Catalysis. Journal of the American Chemical Society, 2014, 136, 6904-6907.	13.7	400
2	Highly Efficient Electroreduction of CO ₂ to Methanol on Palladium–Copper Bimetallic Aerogels. Angewandte Chemie - International Edition, 2018, 57, 14149-14153.	13.8	222
3	Postsynthesis and Selective Oxidation Properties of Nanosized Sn-Beta Zeolite. Journal of Physical Chemistry C, 2011, 115, 3663-3670.	3.1	215
4	The Divergent Synthesis of Nitrogen Heterocycles by Rhodium(I)-Catalyzed Intermolecular Cycloadditions of Vinyl Aziridines and Alkynes. Journal of the American Chemical Society, 2016, 138, 2178-2181.	13.7	148
5	Highly Efficient Electroreduction of CO ₂ to C2+ Alcohols on Heterogeneous Dual Active Sites. Angewandte Chemie - International Edition, 2020, 59, 16459-16464.	13.8	148
6	A highly ordered mesoporous polymer supported imidazolium-based ionic liquid: an efficient catalyst for cycloaddition of CO ₂ with epoxides to produce cyclic carbonates. Green Chemistry, 2014, 16, 4767-4774.	9.0	144
7	Diastereo―and Enantioselective Copper(I)â€Catalyzed Intermolecular [3+2] Cycloaddition of Azomethine Ylides with βâ€Trifluoromethyl β,βâ€Disubstituted Enones. Angewandte Chemie - International Edition, 2016, 55, 6324-6328.	13.8	129
8	Transfer of Chirality in the Rhodium-Catalyzed Intramolecular Formal Hetero-[5 + 2] Cycloaddition of Vinyl Aziridines and Alkynes: Stereoselective Synthesis of Fused Azepine Derivatives. Journal of the American Chemical Society, 2015, 137, 3787-3790.	13.7	109
9	Highly effective photoreduction of CO ₂ to CO promoted by integration of CdS with molecular redox catalysts through metal–organic frameworks. Chemical Science, 2018, 9, 8890-8894.	7.4	95
10	Core/shell-structured TS-1@mesoporous silica-supported Au nanoparticles for selective epoxidation of propylene with H2 and O2. Journal of Materials Chemistry, 2011, 21, 10852.	6.7	88
11	Hollow Metal–Organicâ€Frameworkâ€Mediated Inâ€Situ Architecture of Copper Dendrites for Enhanced CO ₂ Electroreduction. Angewandte Chemie - International Edition, 2020, 59, 8896-8901.	13.8	85
12	Polymer-Bound Chiral Gold-Based Complexes as Efficient Heterogeneous Catalysts for Enantioselectivity Tunable Cycloaddition. ACS Catalysis, 2015, 5, 7488-7492.	11.2	82
13	Hydrophobic Nanosized All-Silica Beta Zeolite: Efficient Synthesis and Adsorption Application. ACS Applied Materials & amp; Interfaces, 2017, 9, 27273-27283.	8.0	77
14	Utilization of CO ₂ as a C1 Building Block in a Tandem Asymmetric A ³ Coupling-Carboxylative Cyclization Sequence to 2-Oxazolidinones. ACS Catalysis, 2017, 7, 8588-8593.	11.2	71
15	Postsynthesis of mesoporous MOR-type titanosilicate and its unique catalytic properties in liquid-phase oxidations. Journal of Catalysis, 2011, 281, 263-272.	6.2	70
16	Design and Synthesis of WJ-Phos , and Application in Cu-Catalyzed Enantioselective Boroacylation of 1,1-Disubstituted Allenes. ACS Catalysis, 2019, 9, 6890-6895.	11.2	70
17	Transition-Metal Catalyzed Carbon-Carbon Couplings Mediated with Functionalized Ionic Liquids, Supported-Ionic Liquid Phase, or Ionic Liquid Media. Current Organic Chemistry, 2009, 13, 1322-1346.	1.6	67
18	Design and Synthesis of TYâ€Phos and Application in Palladiumâ€Catalyzed Enantioselective Fluoroarylation of <i>gem</i> â€Difluoroalkenes. Angewandte Chemie - International Edition, 2020, 59, 22957-22962.	13.8	66

#	Article	IF	CITATIONS
19	Postsynthesis of mesoporous ZSM-5 zeolite by piperidine-assisted desilication and its superior catalytic properties in hydrocarbon cracking. Journal of Materials Chemistry A, 2015, 3, 3511-3521.	10.3	65
20	Preparation of active and robust palladium nanoparticle catalysts stabilized by diamine-functionalized mesoporous polymers. Chemical Communications, 2008, , 6297.	4.1	64
21	Improving the Hydrophobicity and Oxidation Activity of Tiâ^'MWW by Reversible Structural Rearrangement. Journal of Physical Chemistry C, 2008, 112, 6132-6138.	3.1	63
22	Modular Access to the Stereoisomers of Fused Bicyclic Azepines: Rhodium atalyzed Intramolecular Stereospecific Heteroâ€[5+2] Cycloaddition of Vinyl Aziridines and Alkenes. Angewandte Chemie - International Edition, 2015, 54, 15854-15858.	13.8	63
23	Total Hydrogenation of Furfural over Pd/Al ₂ O ₃ and Ru/ZrO ₂ Mixture under Mild Conditions: Essential Role of Tetrahydrofurfural as an Intermediate and Support Effect. ACS Sustainable Chemistry and Engineering, 2018, 6, 6957-6964.	6.7	63
24	Low-Cost Synthesis of Titanium Silicalite-1 (TS-1) with Highly Catalytic Oxidation Performance through a Controlled Hydrolysis Process. Industrial & Engineering Chemistry Research, 2013, 52, 1190-1196.	3.7	62
25	Cesium Carbonate Mediated Borylation of Aryl Iodides with Diboron in Methanol. European Journal of Organic Chemistry, 2013, 2013, 6263-6266.	2.4	60
26	Alkoxysilylation of Ti-MWW lamellar precursors into interlayer pore-expanded titanosilicates. Journal of Materials Chemistry, 2009, 19, 8594.	6.7	59
27	One-pot synthesis of benzamide over a robust tandem catalyst based on center radially fibrous silica encapsulated TS-1. Chemical Communications, 2013, 49, 2709.	4.1	59
28	Regiodivergent Intermolecular [3+2] Cycloadditions of Vinyl Aziridines and Allenes: Stereospecific Synthesis of Chiral Pyrrolidines. Angewandte Chemie - International Edition, 2016, 55, 10844-10848.	13.8	58
29	Highly Efficient Electroreduction of CO ₂ to Methanol on Palladium–Copper Bimetallic Aerogels. Angewandte Chemie, 2018, 130, 14345-14349.	2.0	56
30	Mesopolymer solid base catalysts with variable basicity: preparation and catalytic properties. Journal of Materials Chemistry, 2009, 19, 4004.	6.7	54
31	Selective synthesis of propylene oxide through liquid-phase epoxidation of propylene with H2O2 over formed Ti-MWW catalyst. Journal of Catalysis, 2016, 342, 173-183.	6.2	54
32	Core–Shell-Structured Titanosilicate As A Robust Catalyst for Cyclohexanone Ammoximation. ACS Catalysis, 2013, 3, 103-110.	11.2	51
33	Synthesis of ZSM-5 with hierarchical porosity: In-situ conversion of the mesoporous silica-alumina species to hierarchical zeolite. Microporous and Mesoporous Materials, 2017, 242, 190-199.	4.4	51
34	Axially Chiral Biaryl Monophosphine Oxides Enabled by Palladium/WJ-Phos-Catalyzed Asymmetric Suzuki–Miyaura Cross-coupling. ACS Catalysis, 2020, 10, 1548-1554.	11.2	51
35	Fluorine-planted titanosilicate with enhanced catalytic activity in alkene epoxidation with hydrogen peroxide. Catalysis Science and Technology, 2012, 2, 2433.	4.1	50
36	Direct synthesis of ordered imidazolyl-functionalized mesoporous polymers for efficient chemical fixation of CO ₂ . Chemical Communications, 2015, 51, 682-684.	4.1	49

#	Article	IF	CITATIONS
37	A multifunctional nanotheranostic for the intelligent MRI diagnosis and synergistic treatment of hypoxic tumor. Biomaterials, 2018, 175, 123-133.	11.4	49
38	Hierarchical Metal–Polymer Hybrids for Enhanced CO ₂ Electroreduction. Angewandte Chemie - International Edition, 2021, 60, 10977-10982.	13.8	47
39	Levulinic acid hydrogenation to γ-valerolactone over single Ru atoms on a TiO ₂ @nitrogen doped carbon support. Green Chemistry, 2021, 23, 1621-1627.	9.0	46
40	Enhanced CO ₂ electroreduction <i>via</i> interaction of dangling S bonds and Co sites in cobalt phthalocyanine/ZnIn ₂ S ₄ hybrids. Chemical Science, 2019, 10, 1659-1663.	7.4	45
41	Enantioselective Phosphine-Catalyzed Allylic Alkylations of mix-Indene with MBH Carbonates. Organic Letters, 2017, 19, 6080-6083.	4.6	44
42	Direct Electrochemical Defluorinative Carboxylation of <i>gem</i> -Difluoroalkenes with Carbon Dioxide. Organic Letters, 2020, 22, 8424-8429.	4.6	44
43	Enhancing electroreduction of CO ₂ over Bi ₂ WO ₆ nanosheets by oxygen vacancies. Green Chemistry, 2019, 21, 2589-2593.	9.0	43
44	Boosting the Productivity of Electrochemical CO ₂ Reduction to Multiâ€Carbon Products by Enhancing CO ₂ Diffusion through a Porous Organic Cage. Angewandte Chemie - International Edition, 2022, 61, .	13.8	43
45	Postsynthesis, Characterization, and Catalytic Properties of Aluminosilicates Analogous to MCM-56. Journal of Physical Chemistry C, 2009, 113, 18753-18760.	3.1	42
46	Intermolecular condensation of ethylenediamine to 1,4-diazabicyclo[2,2,2]octane over TS-1 catalysts. Journal of Catalysis, 2009, 266, 258-267.	6.2	39
47	Ru Nanoparticles Entrapped in Mesopolymers for Efficient Liquid-phase Hydrogenation of Unsaturated Compounds. Catalysis Letters, 2009, 133, 63-69.	2.6	39
48	Efficient electrocatalytic reduction of carbon dioxide to ethylene on copper–antimony bimetallic alloy catalyst. Chinese Journal of Catalysis, 2020, 41, 1091-1098.	14.0	39
49	Simultaneous construction of axial and planar chirality by gold/TY-Phos-catalyzed asymmetric hydroarylation. Nature Communications, 2021, 12, 4609.	12.8	39
50	Highly enantioselective Michael addition of 3-arylthio- and 3-alkylthiooxindoles to nitroolefins catalyzed by a simple cinchona alkaloid derived phosphoramide. Chemical Communications, 2014, 50, 15179-15182.	4.1	38
51	Diastereo―and Enantioselective Copper(I)â€Catalyzed Intermolecular [3+2] Cycloaddition of Azomethine Ylides with βâ€Trifluoromethyl β,βâ€Disubstituted Enones. Angewandte Chemie, 2016, 128, 6432-6436.	2.0	38
52	Highly Selective Oxidation of Ethyl Lactate to Ethyl Pyruvate Catalyzed by Mesoporous Vanadia–Titania. ACS Catalysis, 2018, 8, 2365-2374.	11.2	38
53	Palladium-Catalyzed Heck Reaction in the Multi-Functionalized Ionic Liquid Compositions. Catalysis Letters, 2008, 121, 331-336.	2.6	36
54	Cu(II)-Catalyzed Enantioselective β-Boration of β-Trifluoromethyl, β,β-Disubstituted Enones and Esters: Construction of a CF ₃ - and Boron-Containing Quaternary Stereocenter. ACS Catalysis, 2018, 8, 8318-8323.	11.2	36

#	Article	IF	CITATIONS
55	Palladium-Catalyzed Asymmetric Tandem Denitrogenative Heck/Tsuji–Trost of Benzotriazoles with 1,3-Dienes. Journal of the American Chemical Society, 2021, 143, 13010-13015.	13.7	36
56	Boosting nitrate electroreduction to ammonia on NbO _{<i>x</i>} <i>via</i> constructing oxygen vacancies. Green Chemistry, 2022, 24, 1090-1095.	9.0	35
57	Core/shell-structured Al-MWW@B-MWW zeolites for shape-selective toluene disproportionation to para-xylene. Journal of Catalysis, 2011, 283, 168-177.	6.2	34
58	Structural reconstruction: a milestone in the hydrothermal synthesis of highly active Sn-Beta zeolites. Chemical Communications, 2017, 53, 12516-12519.	4.1	34
59	Pd/Xiang-Phos-catalyzed enantioselective intermolecular carboheterofunctionalization under mild conditions. Chemical Science, 2020, 11, 6283-6288.	7.4	34
60	Highly Selective CO ₂ Electroreduction to CO on Cu–Co Bimetallic Catalysts. ACS Sustainable Chemistry and Engineering, 2020, 8, 12561-12567.	6.7	33
61	Hydrothermal synthesis of high-silica mordenite by dual-templating method. Microporous and Mesoporous Materials, 2011, 145, 80-86.	4.4	32
62	Stereoselective defluorinative carboxylation of <i>gem</i> -difluoroalkenes with carbon dioxide. Organic Chemistry Frontiers, 2019, 6, 3678-3682.	4.5	32
63	An efficient synthesis of (E)-nitroalkenes catalyzed by recoverable diamino-functionalized mesostructured polymers. Tetrahedron, 2008, 64, 6294-6299.	1.9	31
64	Understanding the oxidative dehydrogenation of ethyl lactate to ethyl pyruvate over vanadia/titania. Catalysis Science and Technology, 2018, 8, 3737-3747.	4.1	31
65	One-pot synthesized core/shell structured zeolite@copper catalysts for selective hydrogenation of ethylene carbonate to methanol and ethylene glycol. Green Chemistry, 2019, 21, 5414-5426.	9.0	31
66	Electrodeposited Cu–Pd bimetallic catalysts for the selective electroreduction of CO ₂ to ethylene. Green Chemistry, 2020, 22, 7560-7565.	9.0	30
67	Low temperature methanation of CO ₂ over an amorphous cobalt-based catalyst. Chemical Science, 2021, 12, 3937-3943.	7.4	30
68	Mesostructured polymer-supported diphenylphosphine–palladium complex: An efficient and recyclable catalyst for Heck reactions. Catalysis Communications, 2009, 10, 1099-1102.	3.3	29
69	Synthesis of core–shell structured TS-1@mesocarbon materials and their applications as a tandem catalyst. Journal of Materials Chemistry, 2012, 22, 14219.	6.7	29
70	Clean synthesis of acetaldehyde oxime through ammoximation on titanosilicate catalysts. Catalysis Science and Technology, 2013, 3, 2587.	4.1	29
71	Clean synthesis of furfural oxime through liquid-phase ammoximation of furfural over titanosilicate catalysts. Green Chemistry, 2017, 19, 4871-4878.	9.0	29
72	Eco-Friendly and Cost-Effective Synthesis of ZSM-5 Aggregates with Hierarchical Porosity. Industrial & Engineering Chemistry Research, 2017, 56, 13535-13542.	3.7	29

#	Article	IF	CITATIONS
73	Synthesis of Extraâ€Largeâ€Pore Zeolite ECNUâ€9 with Intersecting 14*12â€Ring Channels. Angewandte Chemie International Edition, 2018, 57, 9515-9519.	-13.8	29
74	Selective liquid-phase oxidation of cyclopentene over MWW type titanosilicate. Catalysis Today, 2006, 117, 199-205.	4.4	28
75	Mesoporus MCM-22 Zeolites Prepared through Organic Amine-Assisted Reversible Structural Change and Protective Desilication for Catalysis of Bulky Molecules. ACS Catalysis, 2013, 3, 1892-1901.	11.2	28
76	Hierarchical ZSM-5 nanocrystal aggregates: seed-induced green synthesis and its application in alkylation of phenol with <i>tert</i> butanol. RSC Advances, 2018, 8, 2751-2758.	3.6	28
77	Effect of the coordination environment of Cu in Cu ₂ 0 on the electroreduction of CO ₂ to ethylene. Green Chemistry, 2020, 22, 6340-6344.	9.0	28
78	Palladium/TYâ€Phosâ€Catalyzed Asymmetric Intermolecular αâ€Arylation of Aldehydes with Aryl Bromides. Angewandte Chemie - International Edition, 2021, 60, 18542-18546.	13.8	28
79	Divergent Access to Functionalized Pyrrolidines and Pyrrolines via Iridium-Catalyzed Domino-Ring-Opening Cyclization of Vinyl Aziridines with β-Ketocarbonyls. Organic Letters, 2017, 19, 6526-6529.	4.6	27
80	Effective and Reusable Pt Catalysts Supported on Periodic Mesoporous Resols for Chiral Hydrogenation. Catalysis Letters, 2008, 122, 325-329.	2.6	26
81	A novel acid–base bifunctional catalyst (ZSM-5@Mg ₃ Si ₄ O ₉ (OH) ₄) with core/shell hierarchical structure and superior activities in tandem reactions. Chemical Communications, 2016, 52, 12817-12820.	4.1	26
82	Chirality Transfer in Rhodium(I)-Catalyzed [3 + 2]-Cycloaddition of Vinyl Aziridines and Oxime Ethers: Atom-Economical Synthesis of Chiral Imidazolidines. Organic Letters, 2018, 20, 3587-3590.	4.6	26
83	Pd/GF-Phos-Catalyzed Asymmetric Three-Component Coupling Reaction to Access Chiral Diarylmethyl Alkynes. Journal of the American Chemical Society, 2021, 143, 17983-17988.	13.7	26
84	Hydrothermal synthesis of mesoporous titanosilicate with the aid of amphiphilic organosilane. Journal of Porous Materials, 2010, 17, 399-408.	2.6	25
85	Deboronation-assisted construction of defective Ti(OSi) ₃ OH species in MWW-type titanosilicate and their enhanced catalytic performance. Catalysis Science and Technology, 2020, 10, 2905-2915.	4.1	25
86	Direct synthesis of self-assembled ZSM-5 microsphere with controllable mesoporosity and its enhanced LDPE cracking properties. RSC Advances, 2016, 6, 38671-38679.	3.6	24
87	Highly tunable periodic imidazole-based mesoporous polymers as cooperative catalysts for efficient carbon dioxide fixation. Catalysis Science and Technology, 2019, 9, 1030-1038.	4.1	23
88	An amphiphilic composite material of titanosilicate@mesosilica/carbon as a Pickering catalyst. Chemical Communications, 2018, 54, 7932-7935.	4.1	22
89	An Efficient and Recyclable Mesostructured Polymer-Supported N-Heterocyclic Carbene-Palladium Catalyst for Sonogashira Reactions. Chinese Journal of Catalysis, 2011, 32, 1712-1718.	14.0	21
90	Design and Enantioselective Synthesis of β-Vinyl Tryptamine Building Blocks for Construction of Privileged Chiral Indole Scaffolds. ACS Catalysis, 2017, 7, 4047-4052.	11.2	21

#	Article	IF	CITATIONS
91	Transfer of Chirality in the Rhodium-Catalyzed Chemoselective and Regioselective Allylic Alkylation of Hydroxyarenes with Vinyl Aziridines. Organic Letters, 2017, 19, 2897-2900.	4.6	21
92	Enantioselective carboxylative cyclization of propargylic alcohol with carbon dioxide under mild conditions. Chinese Chemical Letters, 2020, 31, 324-328.	9.0	21
93	Synthesis and formation mechanism of TS-1@mesosilica core–shell materials templated by triblock copolymer surfactant. Microporous and Mesoporous Materials, 2012, 153, 8-17.	4.4	20
94	Hydrothermal synthesis of Sn-Beta zeolites in F ^{â^'} -free medium. Inorganic Chemistry Frontiers, 2018, 5, 2763-2771.	6.0	20
95	Cu(l)â€Mingâ€phos Catalyzed Enantioselective [3+2] Cycloadditions of Glycine ketimines to <i>l²</i> â€Trifluoromethyl Enones. Advanced Synthesis and Catalysis, 2018, 360, 2144-2150.	4.3	19
96	Size-Controlled Growth of Silver Nanoparticles onto Functionalized Ordered Mesoporous Polymers for Efficient CO ₂ Upgrading. ACS Applied Materials & Interfaces, 2019, 11, 44241-44248.	8.0	19
97	Enhanced CO2 electroreduction to ethylene via strong metal-support interaction. Green Energy and Environment, 2022, 7, 792-798.	8.7	19
98	Clean synthesis of biodiesel over solid acid catalysts of sulfonated mesopolymers. Science China Chemistry, 2010, 53, 1481-1486.	8.2	18
99	A Homogeneous Mixture Composed of Vanadate, Acid, and TEMPO Functionalized Ionic Liquids for Alcohol Oxidation by H 2 O 2. ChemCatChem, 2011, 3, 1208-1213.	3.7	18
100	Grubbs-type catalysts immobilized on SBA-15: A novel heterogeneous catalyst for olefin metathesis. Journal of Molecular Catalysis A, 2013, 372, 35-43.	4.8	18
101	Seed-induced synthesis of small-crystal TS-1 using ammonia as alkali source. Chinese Journal of Catalysis, 2015, 36, 1928-1935.	14.0	18
102	Production of alkoxyl-functionalized cyclohexylamines from lignin-derived guaiacols. Green Chemistry, 2021, 23, 8441-8447.	9.0	18
103	Chiral bifunctional bisphosphine enabled enantioselective tandem Michael addition of tryptamine-derived oxindoles to ynones. Chemical Communications, 2019, 55, 9176-9179.	4.1	16
104	Synthesis, Characterization, and Catalytic Properties of Interlayer Expanded Aluminosilicate IEZ-PLS-3. Journal of Physical Chemistry C, 2014, 118, 24662-24669.	3.1	15
105	Au-Catalyzed Formal Allylation of Diazo(thio)oxindoles: Application to Tandem Asymmetric Synthesis of Quaternary Stereocenters. Organic Letters, 2021, 23, 4864-4869.	4.6	15
106	Gold(I)-Catalyzed Enantioselective Cyclopropanation of α-Aryl Diazoacetates with Enamides. Organometallics, 2019, 38, 4036-4042.	2.3	14
107	Synthesis of Sn ₄ P ₃ /reduced graphene oxide nanocomposites as highly efficient electrocatalysts for CO ₂ reduction. Green Chemistry, 2020, 22, 6804-6808.	9.0	14
108	Selective Hydrogenolysis of Lignin Model Compounds to Aromatics over a Cobalt Nanoparticle Catalyst. ACS Sustainable Chemistry and Engineering, 2021, 9, 11862-11871.	6.7	14

#	Article	IF	CITATIONS
109	Highly efficient and clean synthesis of 3,4-epoxytetrahydrofuran over a novel titanosilicate catalyst, Ti-MWW. Green Chemistry, 2006, 8, 78-81.	9.0	13
110	Multifunctional 1,3-diphenylguanidine for the carboxylative cyclization of homopropargyl amines with CO ₂ under ambient temperature and pressure. Chemical Communications, 2019, 55, 14303-14306.	4.1	13
111	Palladium-catalyzed synthesis of 4-cyclohexylmorpholines from reductive coupling of aryl ethers and lignin model compounds with morpholines. Green Chemistry, 2021, 23, 268-273.	9.0	13
112	Synthesis of Functionalized Cyclic Carbonates by Oneâ€Pot Reactions of Carbon Dioxide, Epibromohydrin, and Phenols, Thiophenols, or Carboxylic Acids Catalyzed by Ionic Liquids. European Journal of Organic Chemistry, 2017, 2017, 753-759.	2.4	12
113	Cu(<scp>i</scp>)-catalyzed Michael addition of ketiminoesters to β-trifluoromethyl β,β-disubstituted enones: rapid access to 1-pyrrolines bearing a quaternary all-carbon stereocenter. Organic Chemistry Frontiers, 2017, 4, 1772-1776.	4.5	12
114	Breaking Structural Energy Constraints: Hydrothermal Crystallization of Highâ€Silica Germanosilicates by a Buildingâ€Unit Selfâ€Growth Approach. Chemistry - A European Journal, 2018, 24, 13297-13305.	3.3	12
115	One-step post-synthesis treatment for preparing hydrothermally stable hierarchically porous ZSM-5. Chinese Journal of Catalysis, 2017, 38, 48-57.	14.0	11
116	Freestanding Cobaltâ€Aluminum Oxides on USY Zeolite as an Efficient Catalyst for Selective Catalytic Reduction of NO _{<i>x</i>} . ChemCatChem, 2018, 10, 4074-4083.	3.7	11
117	Two Coexisting Forms of Simple Molecules for Directing Sesqui-Unit-Cell Zeolite Nanosheets. Chemistry of Materials, 2021, 33, 6934-6941.	6.7	11
118	Highly efficient mesoporous polymer supported phosphine-gold(<scp>i</scp>) complex catalysts for amination of allylic alcohols and intramolecular cyclization reactions. RSC Advances, 2018, 8, 1737-1743.	3.6	10
119	Doping Pd/SiO ₂ with Na ⁺ : changing the reductive etherification of Cî€O to furan ring hydrogenation of furfural in ethanol. RSC Advances, 2019, 9, 25345-25350.	3.6	10
120	Highly effective and chemoselective hydrodeoxygenation of aromatic alcohols. Chemical Science, 2022, 13, 1629-1635.	7.4	10
121	Highly Efficient Procedure for the Synthesis of Schiff Bases Using Hydrotalciteâ€like Materials as Catalyst. Chinese Journal of Chemistry, 2009, 27, 1868-1870.	4.9	9
122	Structural diversity of lamellar zeolite Nu-6(1)—postsynthesis of delaminated analogues. Dalton Transactions, 2014, 43, 10492-10500.	3.3	9
123	Enantiodivergent synthesis of 1,2-bis(diphenylphosphino)ethanes <i>via</i> asymmetric [3 + 2]-cycloaddition. Organic Chemistry Frontiers, 2019, 6, 694-698.	4.5	9
124	Alcohol amine-catalyzed CO ₂ conversion for the synthesis of quinazoline-2,4-(1 <i>H</i> ,3 <i>H</i>)-dione in water. RSC Advances, 2020, 10, 34910-34915.	3.6	9
125	Selective photocatalytic aerobic oxidation of methane into carbon monoxide over Ag/AgCl@SiO ₂ . Chemical Science, 2022, 13, 4616-4622.	7.4	9
126	Preparation of Mesoporous Molecular Sieves Al-MSU-S Using Ionic Liquids as Template. Chinese Journal of Chemistry, 2006, 24, 1282-1284.	4.9	8

#	Article	IF	CITATIONS
127	Synthesis of Largeâ€Pore ECNUâ€19 Material (12 × 8â€R) <i>via</i> Interlayerâ€Expansion of HUSâ€2 Lamellar Silicate. Chinese Journal of Chemistry, 2018, 36, 227-232.	4.9	8
128	Surfactant-promoted synthesis of hierarchical zeolite ferrierite nano-sheets. Microporous and Mesoporous Materials, 2021, 312, 110748.	4.4	8
129	ETS-10 Supported Au Nanoparticles for Solvent-Free Oxidation of 1-Phenylethanol with Oxygen. Catalysis Letters, 2011, 141, 860-865.	2.6	7
130	Postsynthesis of high silica beta by cannibalistic dealumination of OSDA-free beta and its catalytic applications. Inorganic Chemistry Frontiers, 2021, 8, 1574-1587.	6.0	7
131	SBAâ€15 Supported Chiral Phosphineâ€Gold(I) Complex: Highly Efficient and Recyclable Catalyst for Asymmetric Cycloaddition Reactions. ChemCatChem, 2020, 12, 4067-4072.	3.7	7
132	Enhancement of Alkene Epoxidation Activity of Titanosilicates by Gasâ€Phase Ammonia Modification. Chinese Journal of Chemistry, 2012, 30, 2205-2211.	4.9	6
133	Liquid-phase oxidation of ethylamine to acetaldehyde oximes over tungsten-doped zeolites. Science China Chemistry, 2017, 60, 942-949.	8.2	6
134	Palladium/TYâ€Phos atalyzed Asymmetric Intermolecular αâ€Arylation of Aldehydes with Aryl Bromides. Angewandte Chemie, 2021, 133, 18690-18694.	2.0	6
135	Synthesis of Ethylâ€4â€ethoxy Pentanoate by Reductive Etherification of Ethyl Levulinate in Ethanol on Pd/SiO ₂ Catalysts. ChemSusChem, 2018, 11, 3796-3802.	6.8	5
136	Hierarchical Metal–Polymer Hybrids for Enhanced CO 2 Electroreduction. Angewandte Chemie, 2021, 133, 11072-11077.	2.0	5
137	Preparation of trimetallic electrocatalysts by one-step co-electrodeposition and efficient CO ₂ reduction to ethylene. Chemical Science, 2022, 13, 7509-7515.	7.4	5
138	K ⁺ located in 6-membered rings of low-silica CHA enhancing the lifetime and propene selectivity in MTO. Catalysis Science and Technology, 2021, 11, 6234-6247.	4.1	4
139	Efficient synthesis of bioetheric fuel additive by combining the reductive and direct etherification of furfural in one-pot over Pd nanoparticles deposited on zeolites. Green Energy and Environment, 2023, 8, 519-529.	8.7	4
140	A highly efficient procedure for the oxathioacetalization of carbonyl compounds under solvent-free conditions. Science in China Series B: Chemistry, 2009, 52, 2166-2170.	0.8	3
141	Aluminated hierarchical silicalite-2 particles: Catalyst with remarkably increased lifetime for methanol to hydrocarbons. Catalysis Communications, 2016, 86, 139-142.	3.3	3
142	Copper-catalyzed cyclization reaction: synthesis of trifluoromethylated indolinyl ketones. Chemical Communications, 2021, 57, 4448-4451.	4.1	3
143	Expanded titanosilicate MWW-related materials synthesized from a boron-containing precursor as an efficient catalyst for cyclohexene oxidation. Microporous and Mesoporous Materials, 2021, 327, 111437.	4.4	3
144	Controllably Confined ZnO on USY Zeolites (USY@ZnO/Al ₂ O ₃) as Efficient Lewis Acid Catalysts for Baeyer–Villiger Oxidation. Chemistry - an Asian Journal, 2018, 13, 1213-1222.	3.3	2

#	Article	IF	CITATIONS
145	Efficient Electrocatalytic Reduction of Levulinic Acid to Valeric Acid on a Nanocrystalline PbOâ€In ₂ O ₃ Catalyst. ChemistrySelect, 2022, 7, .	1.5	2
146	A neutral Cu-based MOF for effective quercetin extraction and conversion from natural onion juice. RSC Advances, 2019, 9, 33716-33721.	3.6	1
147	Preparation of a cost-effective Ni–Ag bimetallic catalyst for hydrodehalogenation of aryl halides under mild conditions. New Journal of Chemistry, 2022, 46, 12169-12176.	2.8	1